

# Radiative shock waves produced from implosion experiments at the National Ignition Facility

National Ignition Campaign Team  
Arthur Pak  
Lawrence Livermore National Laboratory



Presented to:  
**2013 National Ignition Facility and Jupiter Laser Facility Users Group Meeting**

## Collaborators

---

**L. Divol<sup>1</sup>, G. Gregori<sup>5</sup>, S. Weber<sup>1</sup>, L. J. Atherton<sup>1</sup>, D. Callahan<sup>1</sup>, E. Dewald<sup>1</sup>, T. Doeppner<sup>1</sup>, M. J. Edwards<sup>1</sup>, S. Glenn<sup>1</sup>, D. Hicks<sup>1</sup>, N. Izumi<sup>1</sup>, O. S. Jones<sup>1</sup>, S. Khan<sup>1</sup>, J. D. Kilkenny<sup>4</sup>, G. A. Kyrala<sup>3</sup>, J. L. Kline<sup>3</sup>, J. D. Lindl<sup>1</sup>, O. L. Landen<sup>1</sup>, S. Lepape<sup>1</sup>, T. Ma<sup>1</sup>, A. MacPhee<sup>1</sup>, B. J. MacGowan<sup>1</sup>, A. J. MacKinnon<sup>1</sup>, L. Masse<sup>6</sup>, N. B. Meezan<sup>1</sup>, E. Moses<sup>1</sup>, R. E. Olson<sup>2</sup>, J. E. Ralph<sup>1</sup>, H.-S. Park<sup>1</sup>, B.A. Remington<sup>1</sup>, J. S. Ross<sup>1</sup>, V. Smalyuk<sup>1</sup> and S. H. Glenzer<sup>1</sup>**

**<sup>1</sup>Lawrence Livermore National Laboratory, Livermore, CA, USA**

**<sup>2</sup>Sandia National Laboratories, Albuquerque, NM, USA**

**<sup>3</sup>Los Alamos National Laboratory, Los Alamos, NM, USA**

**<sup>4</sup>General Atomics, San Diego, CA, USA**

**<sup>5</sup>Oxford University, Oxford , UK**

**<sup>6</sup>CEA, DAM, DIF, F-91297 Arpajon, France**



## Summary

---

- Radiative shock waves observed from integrated ignition experiments performed with cryogenic thermonuclear DT fuel
  - Stagnation pressure  $> 100$  Gbar with convergence ratio  $\sim 30$  and fuel densities reaching  $> 500\text{g/cc}$
- 200 - 300 ps after peak compression, the x-ray emission from a spherically expanding radiative shock wave is observed.
  - Expansion velocity of 300 km/s
  - Measured  $\sim 9$  keV x-ray luminosity of  $\sim 3$  GW
  - Simulations are consistent with observed velocity and luminosity and indicate that the observed shock is radiative.

**Capsule implosions in NIF hohlraums produce radiative shocks that are of interest for astrophysics and implosion performance**

# Radiative shocks are of interest to a variety of astrophysical phenomena and have been created using energetic high power lasers

---

Radiative shocks –

- During a supernova within a stellar interior.
- Early time ballistic expansion of ejecta interacting with stellar atmosphere.
- Supernova remnants.
- Bow shocks of high velocity stellar jets.

Previous experimental work on radiative shocks in laser driven shock tubes:

J.C. Bozier *et al.* (1986), P.A. Keiter *et al.* (2002), S. Bouquet *et al.* (2004), Reighart *et al.* (2006), M. Gonzalez *et al.* (2006), R. P. Drake *et al.* (2011), C. C. Kuranz B13 11:30 am, Monday.

Previous work on laser produced blast waves:

J. Grun *et al.* (1991), K. Keilty *et al.* (2000), T. Ditmire *et al.* (2000), K. Shigemori *et al.* (2000), J. Edwards *et al.* (2001), A.D. Edens *et al.* (2004-5), J.F. Hansen *et al.* (2006), A. S. Moore (2008)

Laboratory astrophysics review:

B. A. Remington, R. P. Drake, D. D. Ryutov Rev. Mod. Phys. Vol. 78. No 3 (2006)

This work describes and details a radiative shock driven by the expansion of a dense shell ( $\rho_0 \sim 500$  g/cc) of material into a hot (300 eV) dense (1 g/cc) in falling medium.

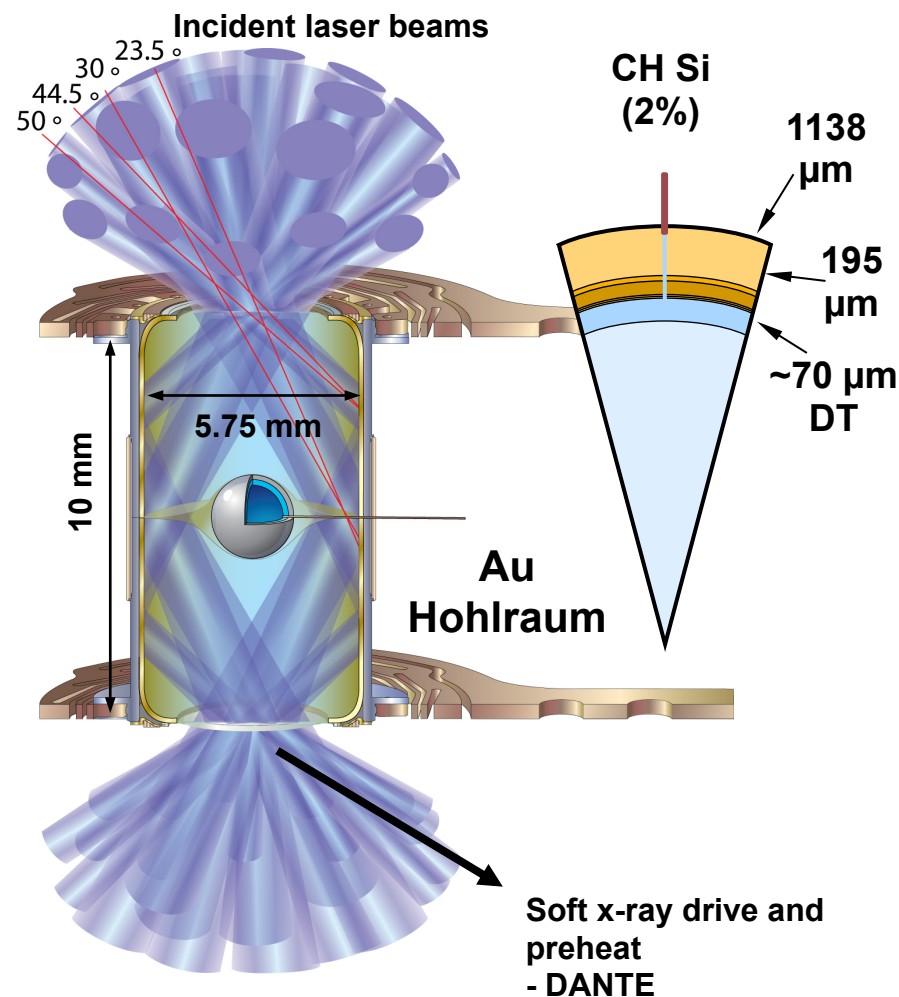


# Indirect drive implosions on the National Ignition Facility

## Brief overview of the National Ignition Facility (NIF)



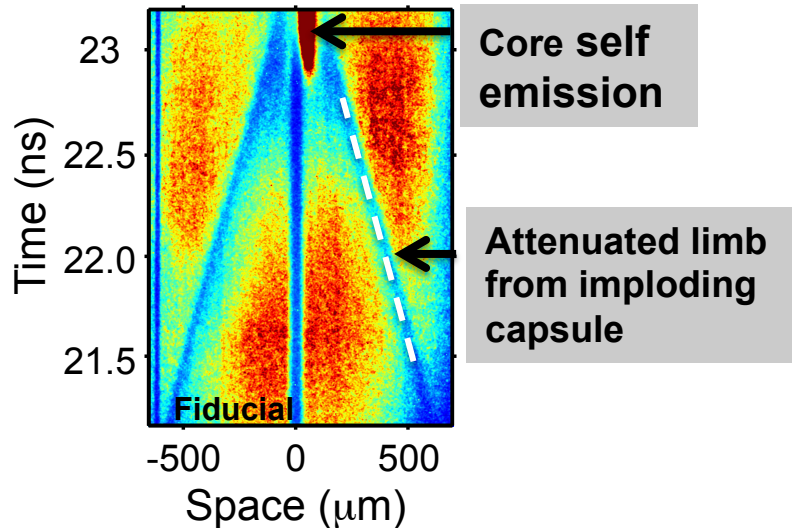
- 192 laser beams
- 1.9 MJ of energy at 351 nm.
- 500 TW of power.
- Suite of x-ray and nuclear diagnostics.
- State of the art target fabrication and positioning.



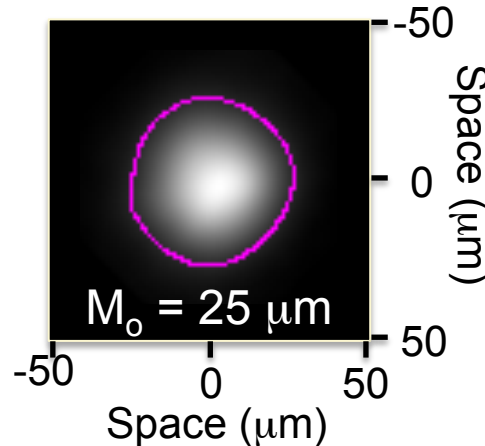
Soft x-ray drive ablates capsule surface creating the pressure which drives the implosion

# Multiple diagnostics and different experimental platforms are used to measure the conditions of the implosion

Con. A. platform measures a remaining shell mass of  $450 \mu\text{g}$  imploding at  $300 \text{ km/s}$



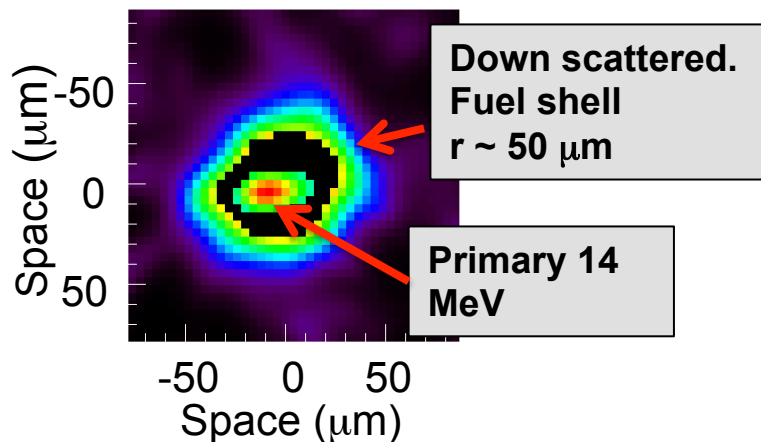
Time integrated x-ray pinhole images measure energy emitted at  $\sim 9 \text{ keV}$



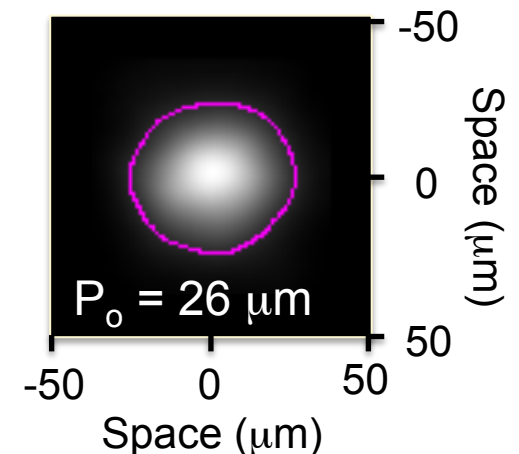
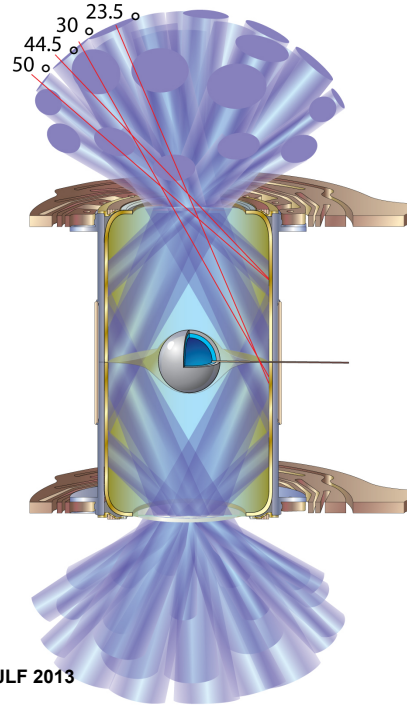
- Neutron yield  $\sim 5 \times 10^{14}$
- Core  $T_{\text{ion}} \sim 2\text{-}4 \text{ keV}$
- Core radius  $\sim 25 \mu\text{m}$
- $\tau_{\text{BW}} \sim 200 \text{ ps}$

$n_i$  (Yield,  $T_{\text{ion}}$ , Volume,  $\tau_{\text{BW}}$ )

Neutron imager shows dense fuel shell surrounding hot core

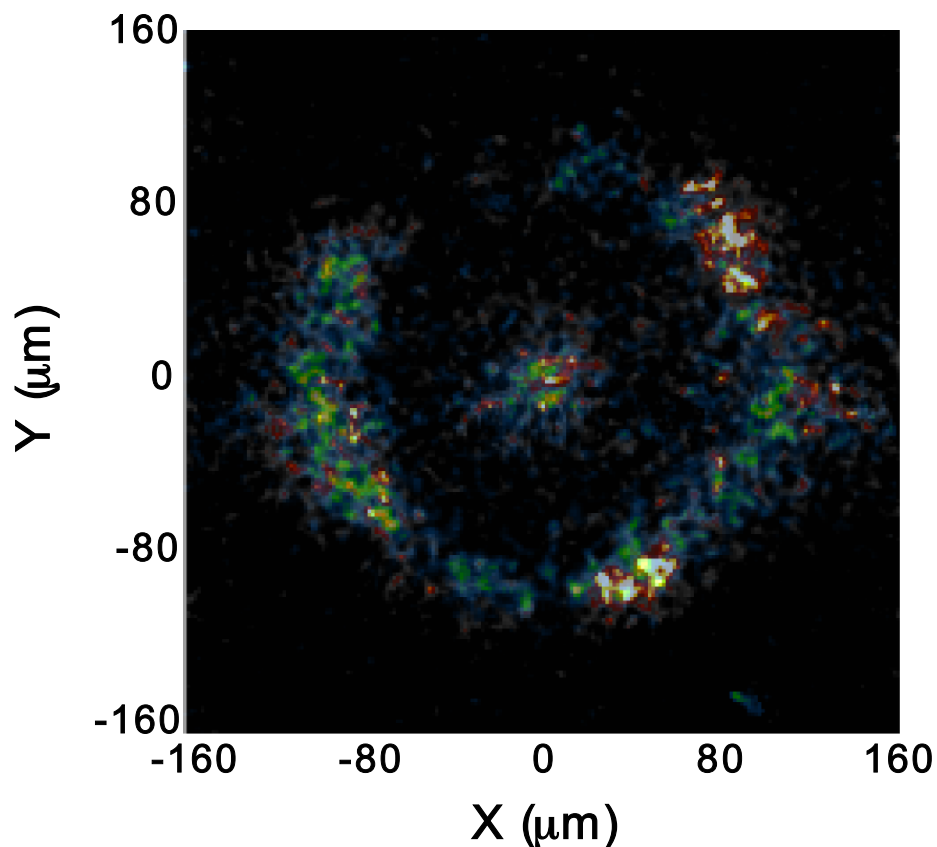


$$P_{\text{HS}} = (n_i + n_e) K T_i \approx 100 \text{ Gb}$$



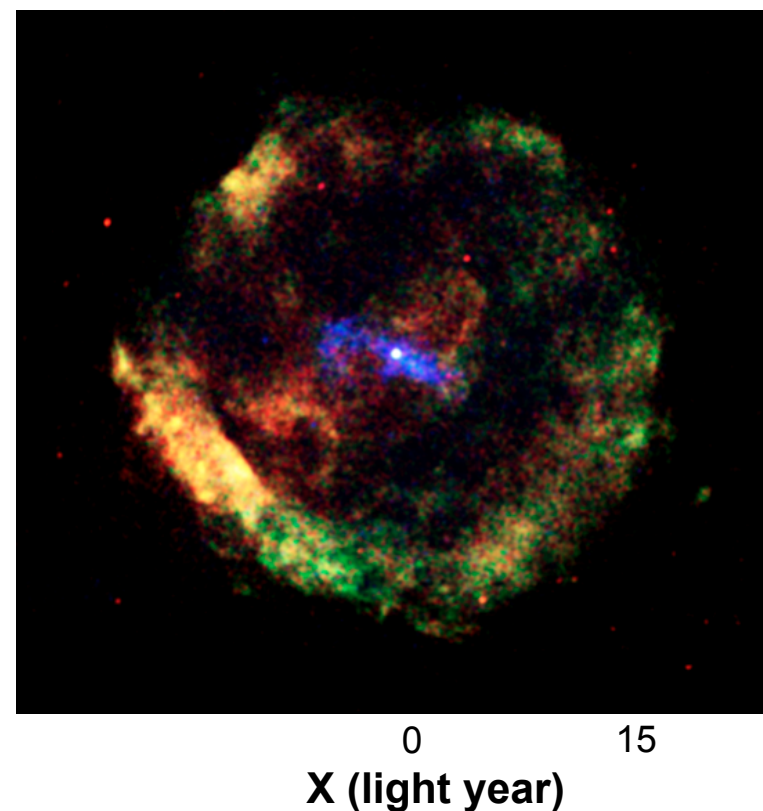
# X-ray emission from a spherical blast wave is observed at NIF and in astrophysical events

X-ray emission at  $t = 300$  ps after peak compression



NIF implosions with Gbar stagnation pressures create a strongly emitting out going shock wave ( $\sim 9$  keV)

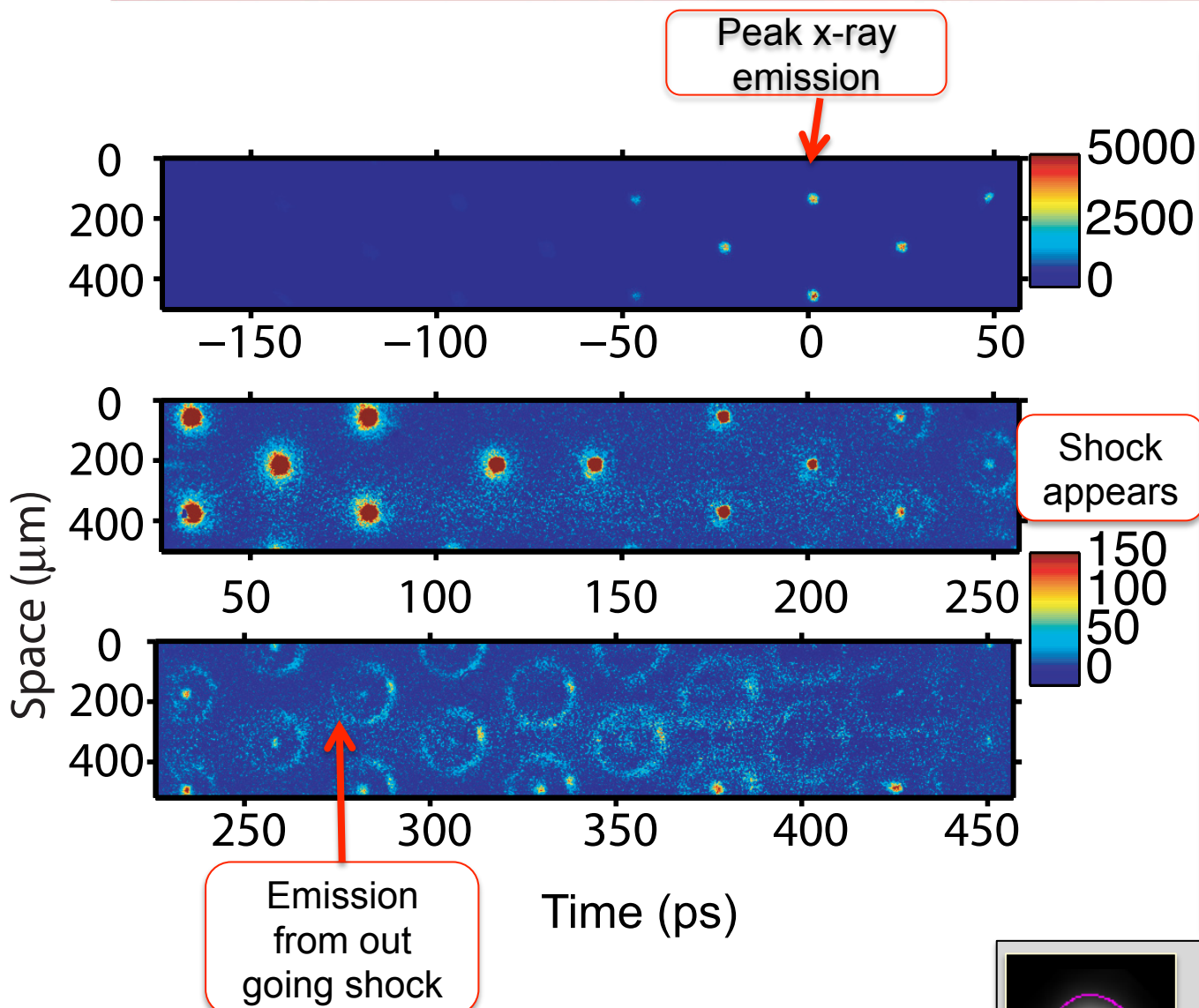
Supernova remnant G11.2-0.3 at  $t = 2600$  years after peak compression



In Chandra's X-ray image. A shell of heated gas from the outer layers of the exploded star surrounds the pulsar and emits lower-energy X-rays

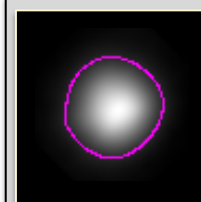


# X-ray emission is temporally and spatially resolved using gated micro channel plate detector



Emission from out going shock wave observed  $\sim 200$  ps after peak x-ray emission

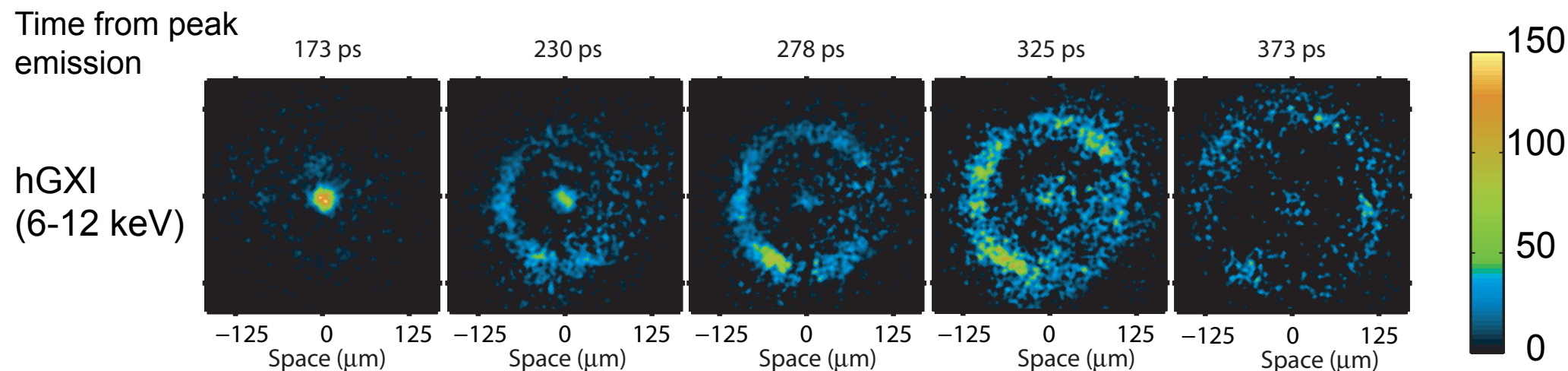
- Temporal gain width 40 – 100 ps.
- Spatial resolution  $\sim 10 \mu\text{m}$ .
- Flat fielded response of detector.
- Measure emission vs. time, gives burn width.
- Emission from shock observed for  $\sim 200$  ps.



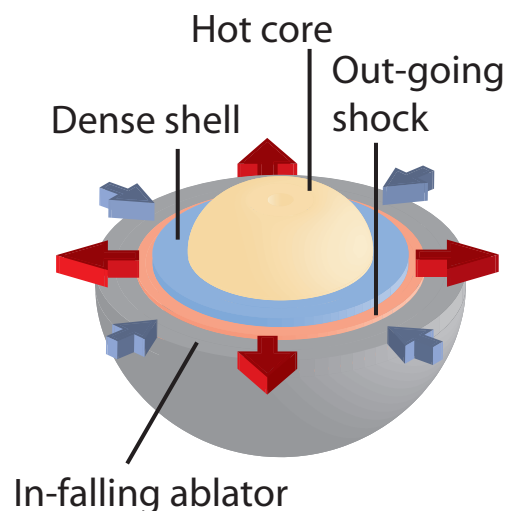
Gated detector cross calibrated using image plate emission data (J / counts).

# X-ray emission from outward going shock observed

Ring of x-ray emission appears 200 ps after peak x-ray emission



At stagnation the hot core and dense shell of DT fuel are surround by in-falling ablator plasma.



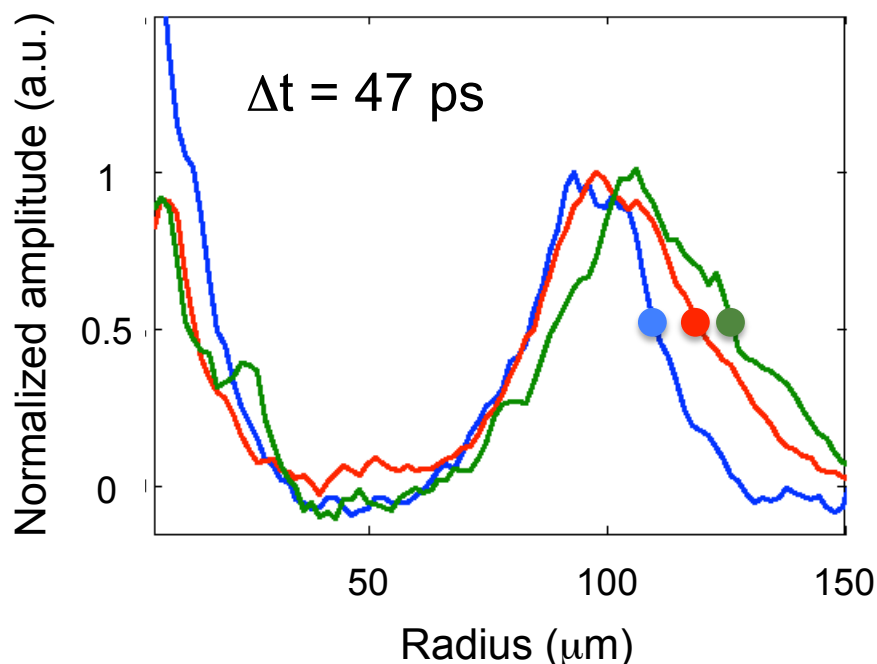
After stagnation a shock propagates outwards ahead of the expanding compressed Material.

# Shock velocity observed to be ~280-330 km/s

Radius of shock found by tracking edge of emission.

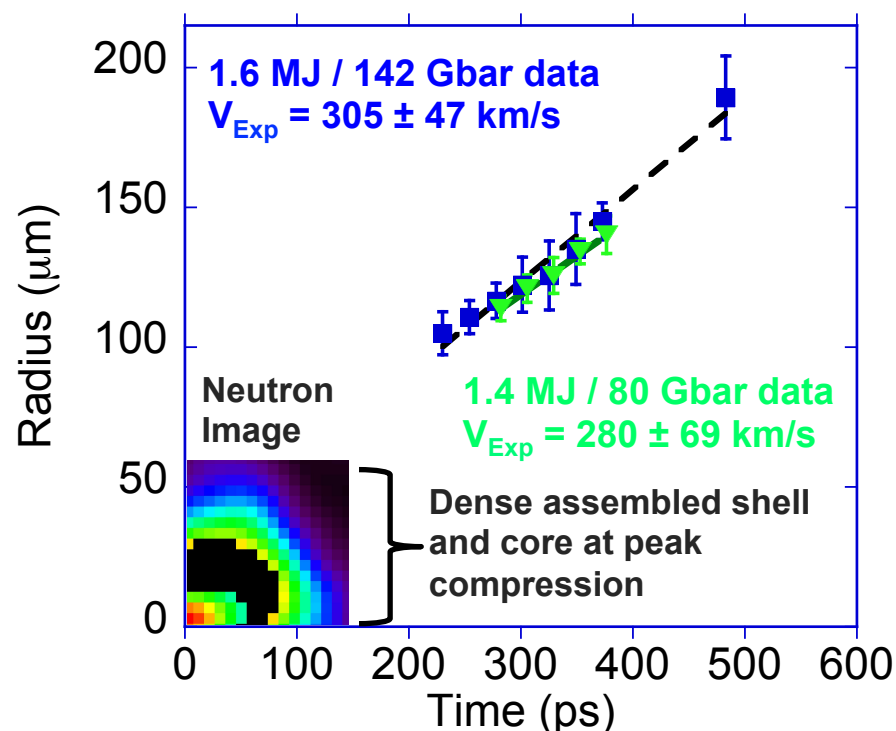
Velocity approximately constant over 2x in radius

Normalized radial emission profiles



- Thin shell of emission indicative of radiative shock.
- Width of emission  $\sim 10 \mu\text{m}$  (resolution element)  $\propto v\tau = 30 \mu\text{m}$  with  $\tau \sim 100 \text{ ps}$  and  $v = 300 \text{ km/s}$ .

Shock radius vs. time



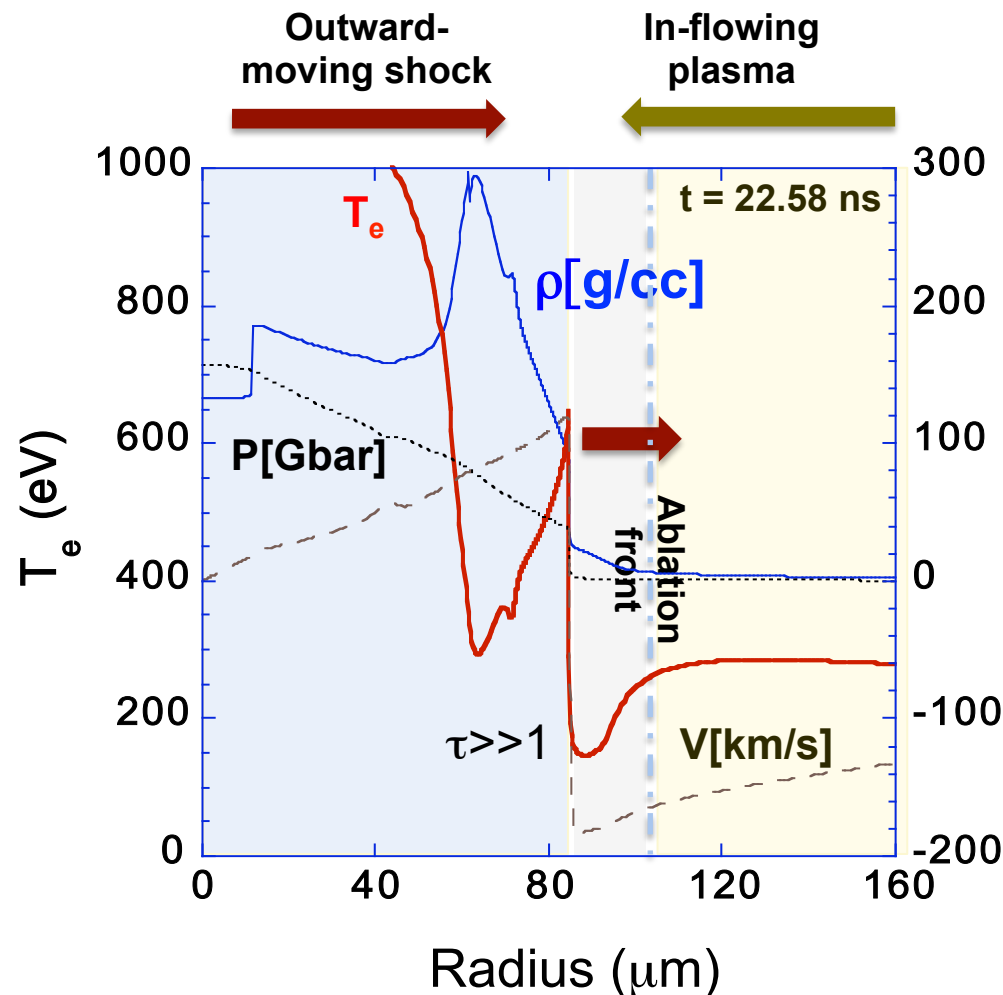
- Emission drops below detectable level  $\sim 500 \text{ ps}$  after peak emission.
- Strong shock still propagating.



# Radiation hydrodynamic simulations show x-ray emission becomes visible as shock propagates into optically thinner ablation front.

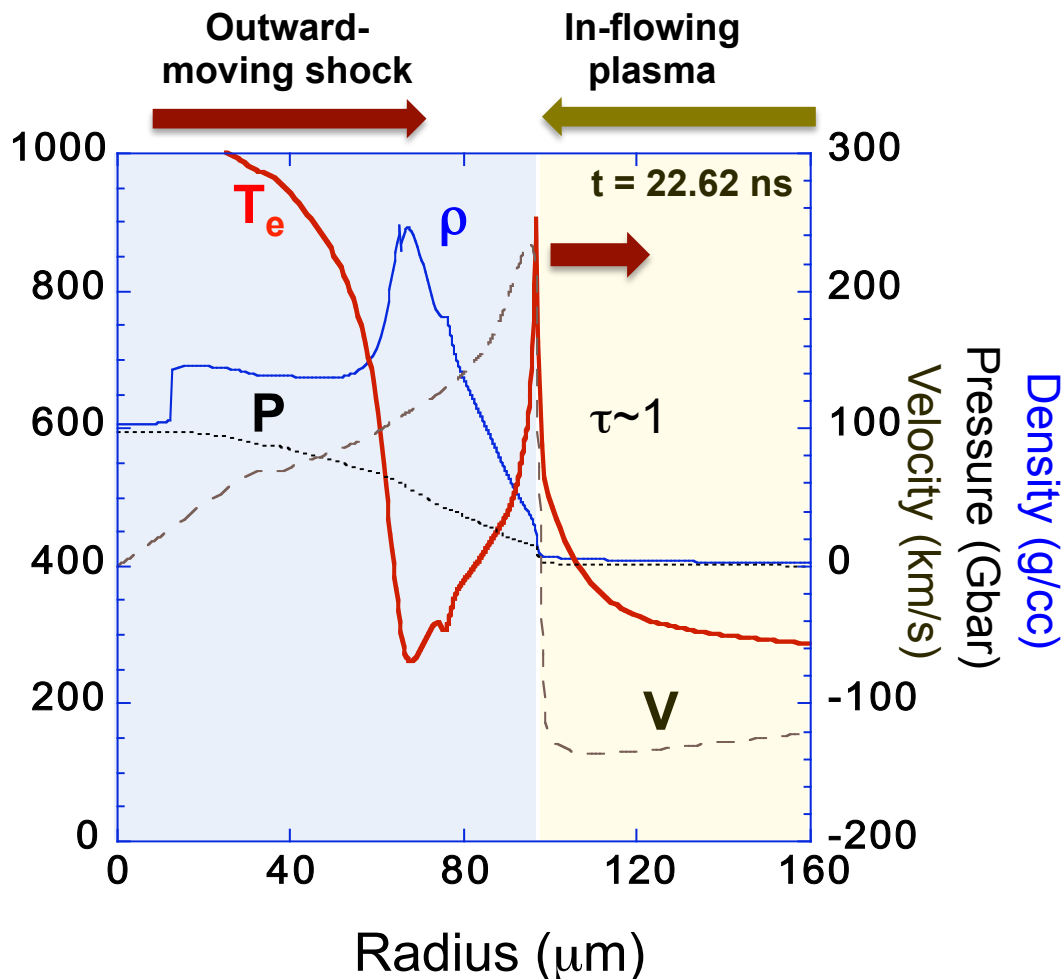
Shock propagates through dense shell and into ablation front

Temperature of the shocked material rises to .9 keV at ablation front



Dense shell expanding outwards against in falling ablator

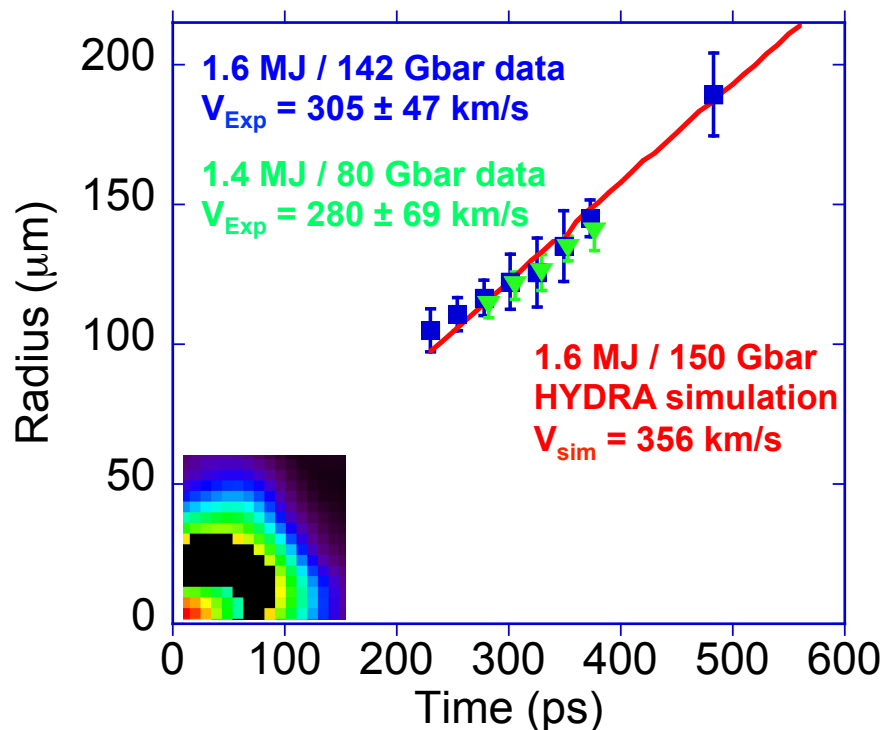
NIF / JLF 2013



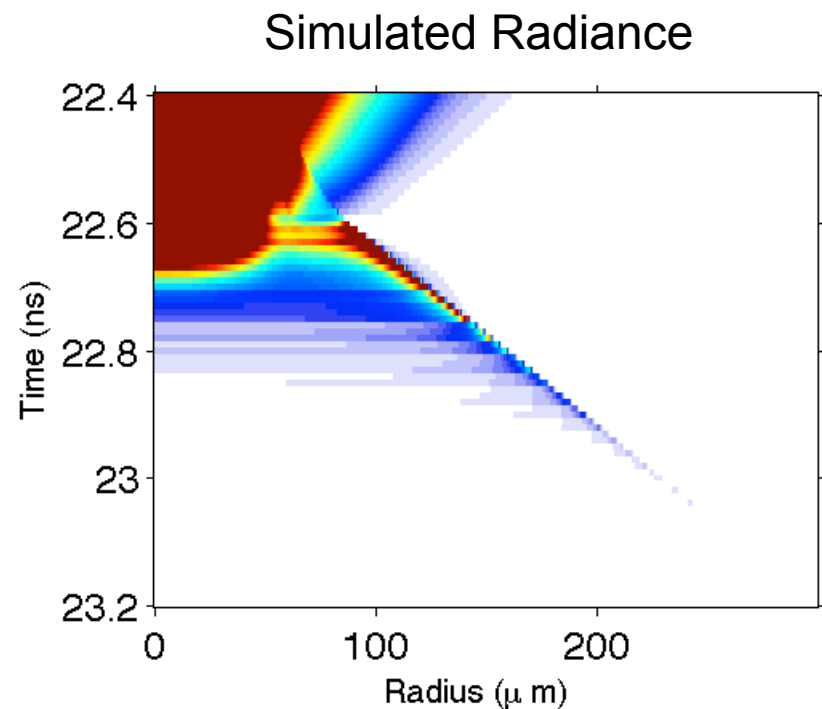
Density / Temp. of upstream material drops / rises at ablation front.

# Simulations of 150 Gbar implosions indicate similar shock expansion velocities and the formation of a strongly radiating shock

Simulations reproduce velocity of observed emission



Simulations show a limb brightened ring of emission

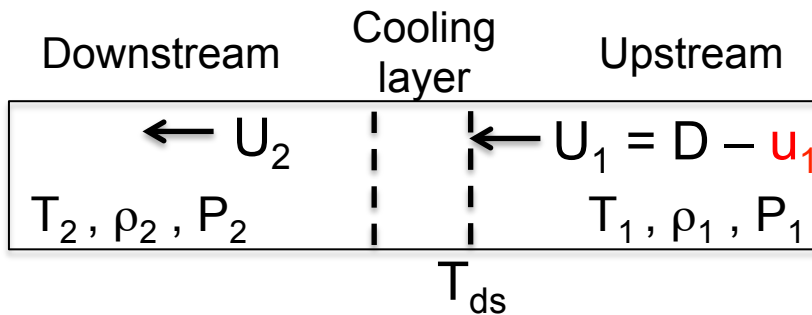


- Simulations show constant velocity in time out to at least 1500 ps.
- Ablation front radius depends on shock velocity and shell width.
- Initial simulations require temporal offset.

Simulations show a ring of emission expanding at nearly constant velocity.

# Post shock temperature is higher for the measured shock velocity due to in flowing material and hohlraum drive

In falling material increases post shock temperature



$$U_1 = D - u_1 = \text{shock velocity} - \text{initial velocity}$$

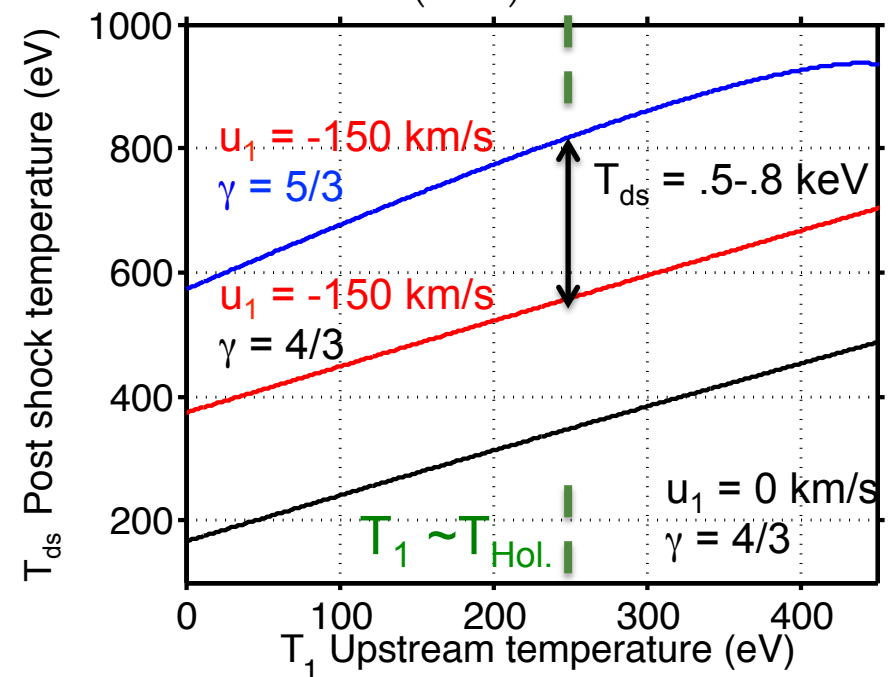
$$U_1 = 450 \text{ km/s} = [300 - (-150)] \text{ km/s}$$

$$T_{ds} = \frac{A}{k_b(1+Z)} \frac{(\gamma-1)}{(\gamma+1)^2} 2(D - u_1)^2$$

Hugoniot relations  
( $T_1 \sim 0$ ,  
 $P_2 \gg P_1$ )

Finite upstream temperature increases post shock temperature

$$T_{ds} \approx \frac{2(\gamma-1)}{R(\gamma+1)^2} U_1^2 + T_1 \quad (P_2 \gg P_1)$$



CH,  $Z_H = 1$ ,  $Z_c = 6$

For a  $D = 300 \text{ km/s}$  an upstream velocity of  $-150 \text{ km/s}$  increases the shock temperature by  $\sim 2X$

Hohlraum drive adds energy preheating upstream material  $T_1$  to  $\sim 250 \text{ eV}$



# Material pressure greater than radiation pressure while radiative energy flux is approximately equal to in-flowing material energy flux.

Upstream and downstream conditions estimated at ablation front

Simulations indicate the formation of a 'super critical' shock

In falling ablation front  $\rho_1$

$$\sigma T_R^4 = 4\rho_1 c_s^3 \quad \rho_1 = 1 \text{ g/cc}$$

$$T_R = 250 \text{ eV}$$

$$c_s = \sim 115 \text{ km/s isothermal}$$

Shock parameters

$$U_1 = 485 \text{ km/s}$$

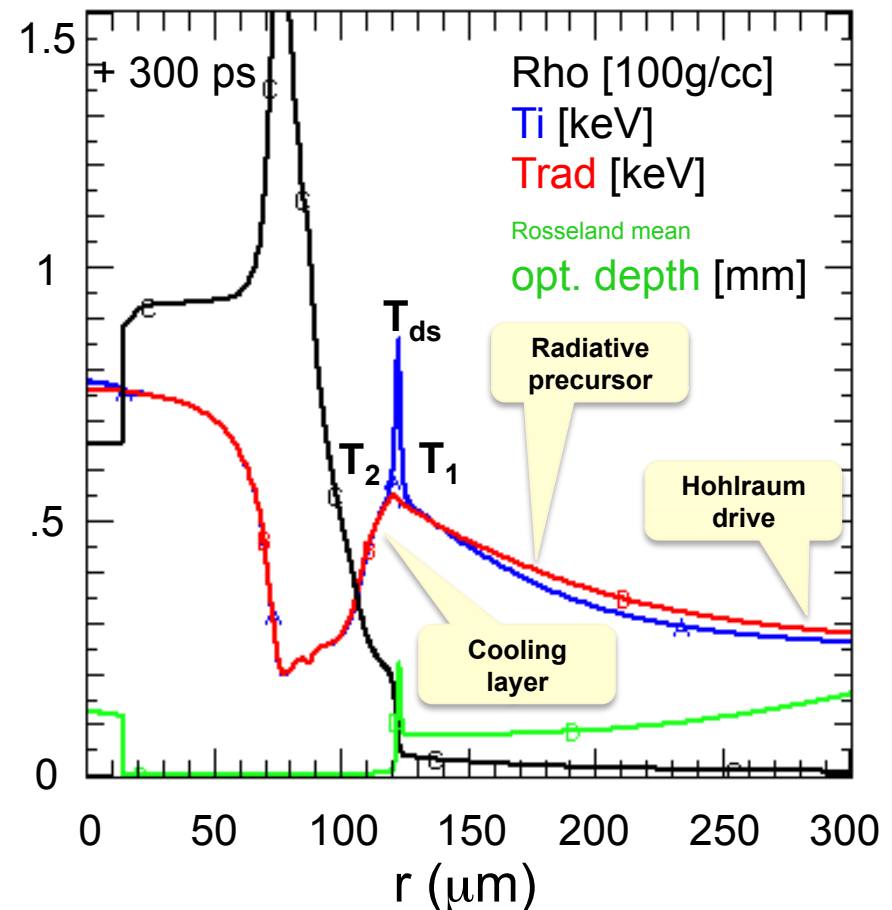
$$T_2 = 350 \text{ eV} *$$

$$\frac{\rho_2}{\rho_1} \approx 10 *$$

$$\frac{P_{Mat.}}{P_{Rad.}} = \frac{(N_i + N_e)k_b T_2}{\left(\frac{4\sigma T_{ds}^4}{3c}\right)} \approx \frac{1.5 \text{ Gb}}{.03 \text{ Gb}} \approx 50$$

$$* \quad \frac{F_{Rad.}}{F_{mat.}} = 4 \frac{\sigma T_2^4}{\rho_1 U_1^3} \approx 1$$

Radiative flux will modify shock front structure.



Supercritical:  $T_2 = T_1$ ;  $T_{ds} = (3 - \gamma)T_1$

# Shock velocity indicates the energy imparted and generated by the implosion.

The observed shock velocity is indicative of energy deposited into the implosion.

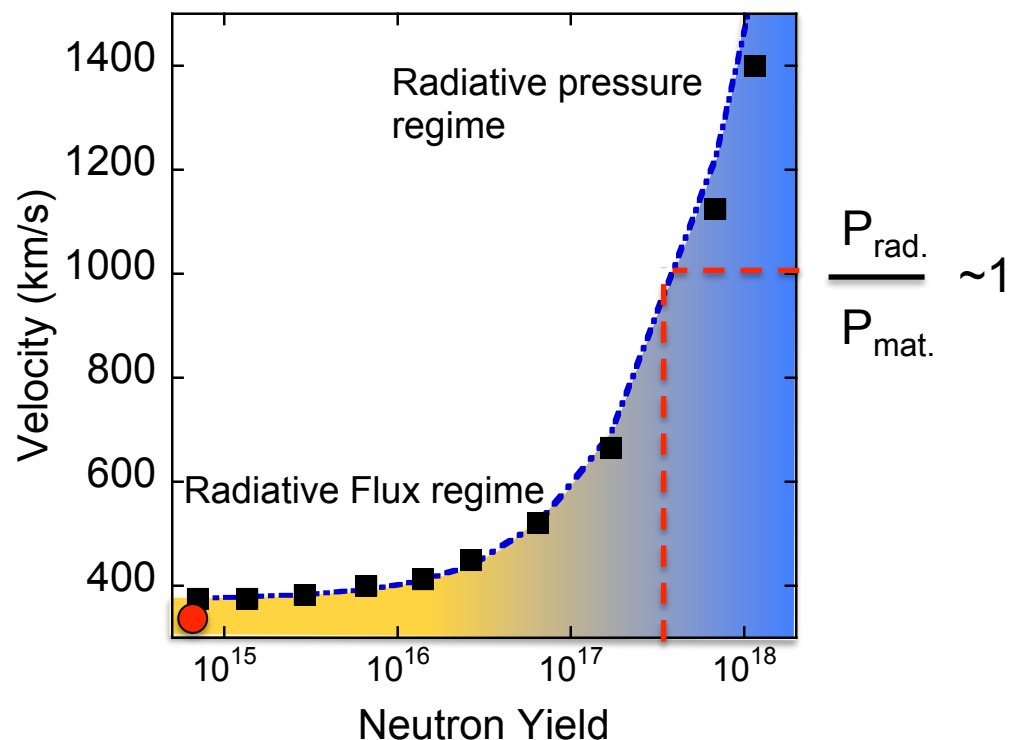
$u_2$  proportional to energy deposited into implosion.

$$u_2 = D - \frac{\rho_1}{\rho_2} (D - u_1) \quad \begin{array}{l} D, u_2, u_1 \text{ lab frame} \\ \text{shock, down / up} \\ \text{stream velocities} \end{array}$$

$$D = \frac{\left( u_2 - \frac{\rho_1}{\rho_2} u_1 \right)}{\left( 1 - \frac{\rho_1}{\rho_2} \right)} \propto \sqrt{\frac{2E}{m_{imp.}}}$$

- $\alpha$  heating or partial burn will add energy to system.
- Diagnosing the shock velocity indicates how much additional energy released.

Radiative pressure regime can be accessed as implosion performance improves

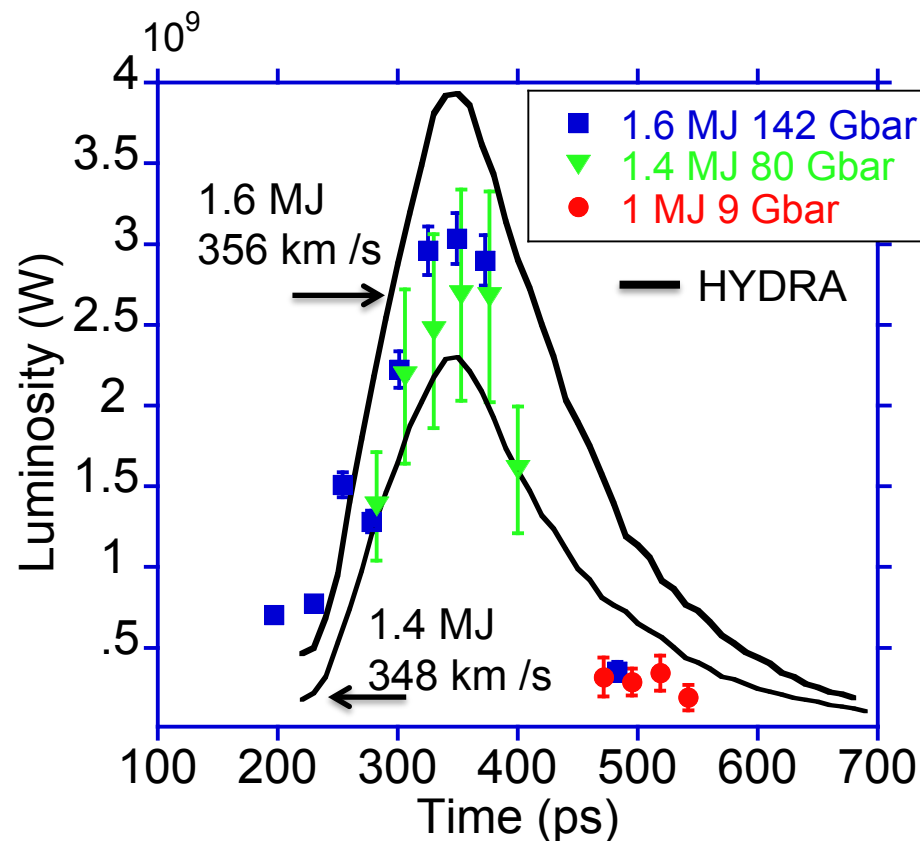
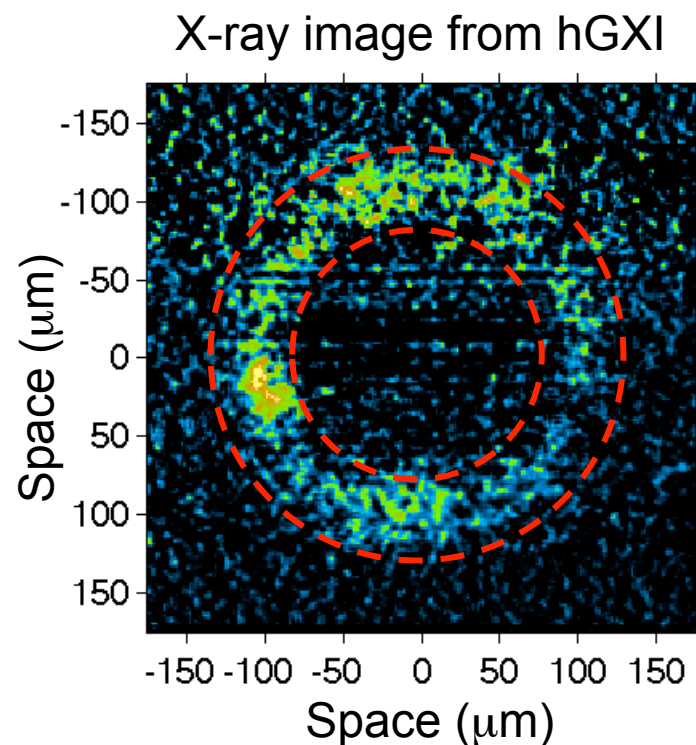


The shock velocity will increase as cryogenic implosion performance improves allowing access to the radiative pressure regime.

# The measured luminosity at $\sim 9$ keV incident onto detector is in agreement with simulated luminosity

Time averaged power measured using cross calibration from I.P.

Agreement between observed and simulated luminosity at  $\sim 9$  keV



Peak luminosity of 3 GW at 9 keV

- Time averaged over 100 ps.
- Same filtering on hGXI as on I.P.
- Similar spectral response.

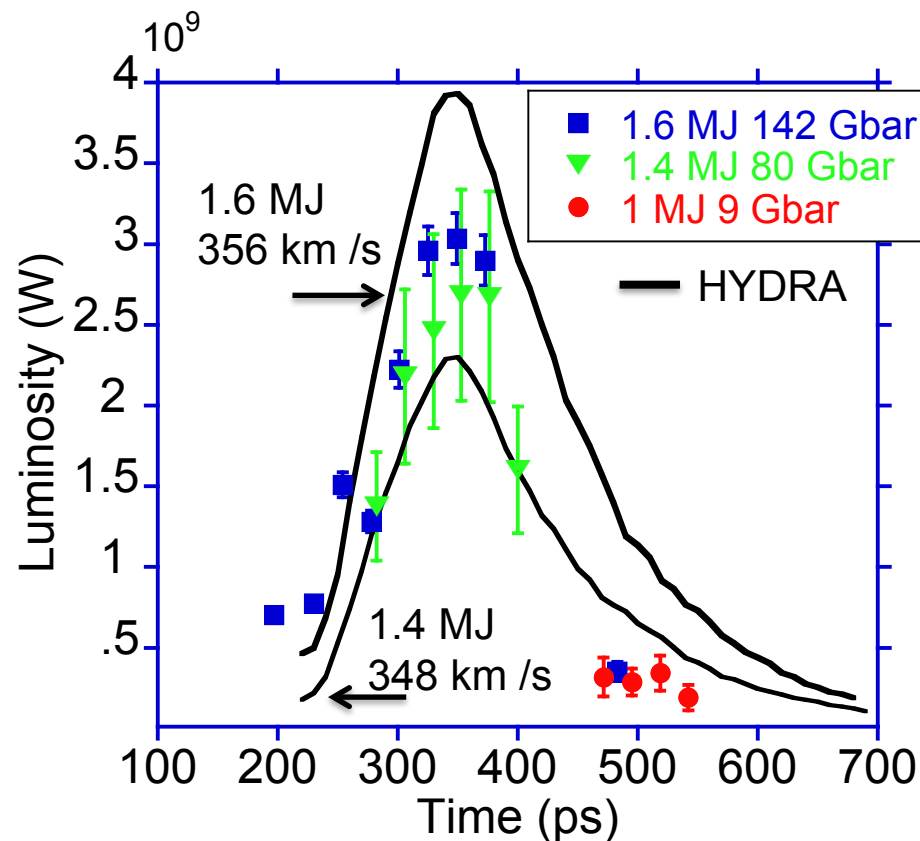
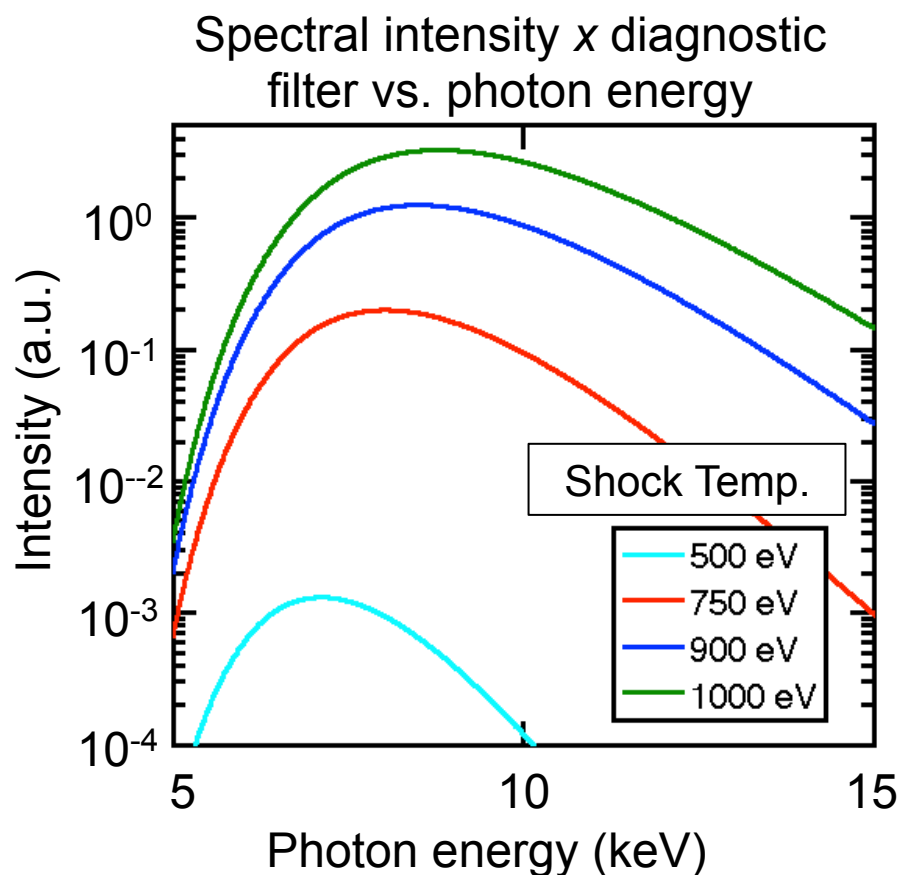
- Simulations show luminosity  $> 1$  keV = 2.25 TW ( $2.25 \times 10^{19}$  ergs)



# The detected luminosity is strongly sensitive to post shock temperature

Diagnostic filtering focuses the measurement on the spectral tail

Agreement between observed and simulated luminosity at  $\sim 9$  keV



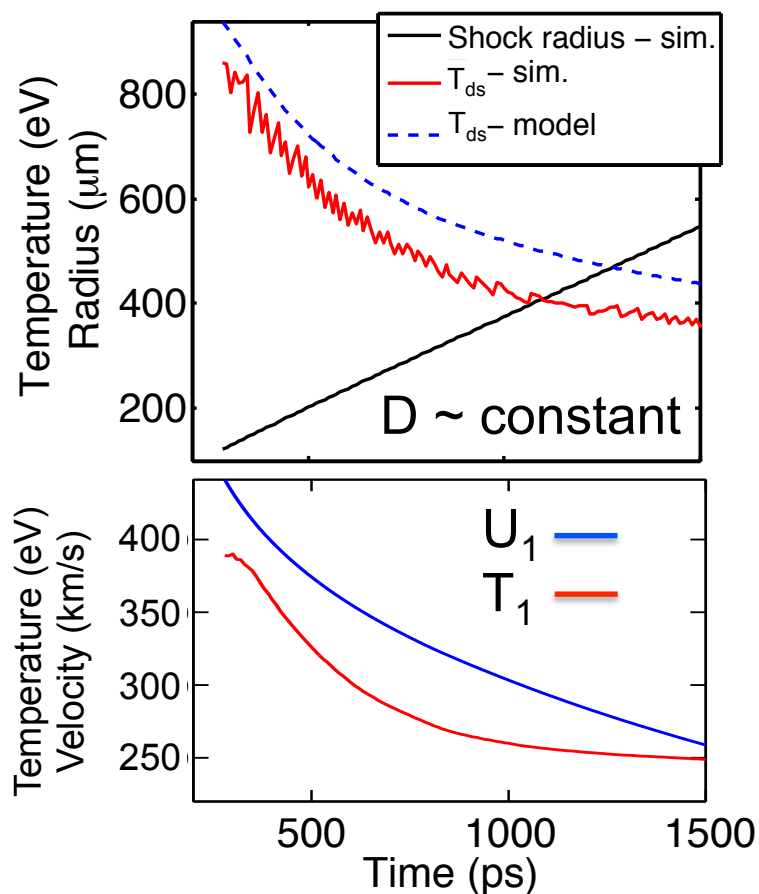
- $10\% \Delta T \approx 60\% \Delta \text{Spec. Int.}$
- Filtering focuses measurement at  $E \gg kT_{\text{shock}}$

- Simulations show luminosity  $> 1$  keV = 2.25 TW ( $2.25 \times 10^{19}$  ergs)

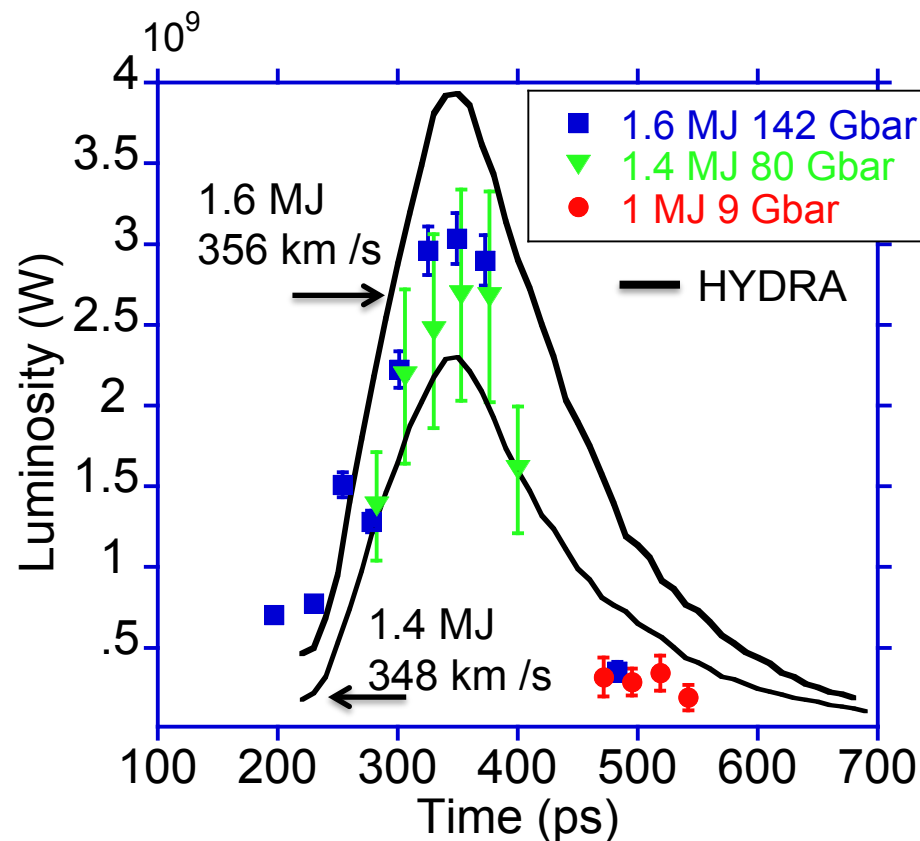
# The measured luminosity at ~ 9 keV incident onto detector is in agreement with simulated luminosity

Luminosity drops with time as  $U_1$  and  $T_1$  decrease.  $D(t) \sim \text{constant}$ .

$$T_{ds} \approx \frac{2(\gamma-1)}{R(\gamma+1)^2} \underbrace{(D-u_1)^2}_{U_1} + T_1$$



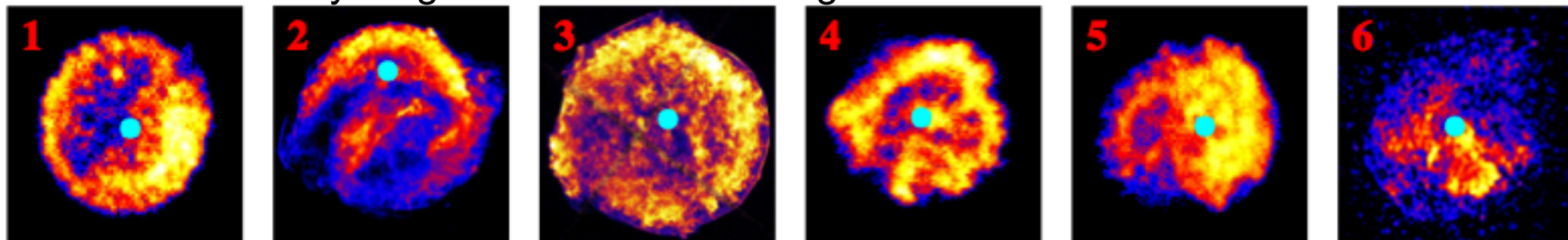
Agreement between observed and simulated luminosity at ~9 keV



- Simulations show luminosity > 1 keV = 2.25 TW ( $2.25 \times 10^{19}$  ergs)

# Current experiment offers and opportunity to study the evolution of spherical radiative shock waves

X-ray emission is being used to constrain the morphology and composition of young SNR and surrounding circumstellar medium

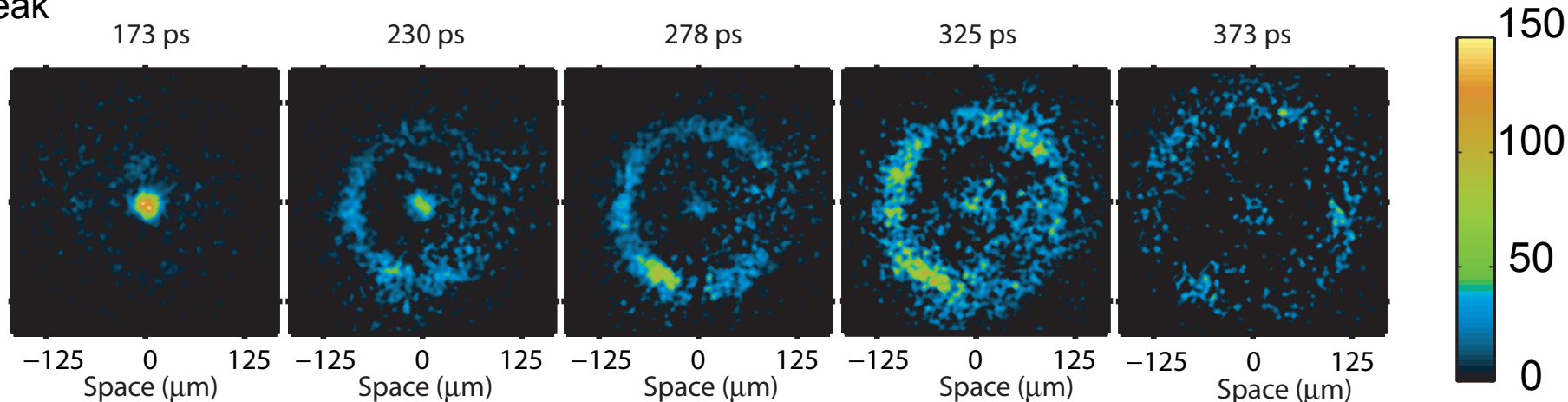


Chandra .5-2.1 keV emission from 6 different young supernova.

Laboratory explosion. Radiative shock wave interacting with CH plasma.

Time from peak emission

hGXI  
(6-12 keV)



# Different astrophysical regimes can be studied by modifying the target and diagnostics

Shocks with higher  $F_{\text{rad}} / P_{\text{rad}}$  can be created by modifying targets

- Directly driven targets.
- $\alpha$  heating deposition of energy.

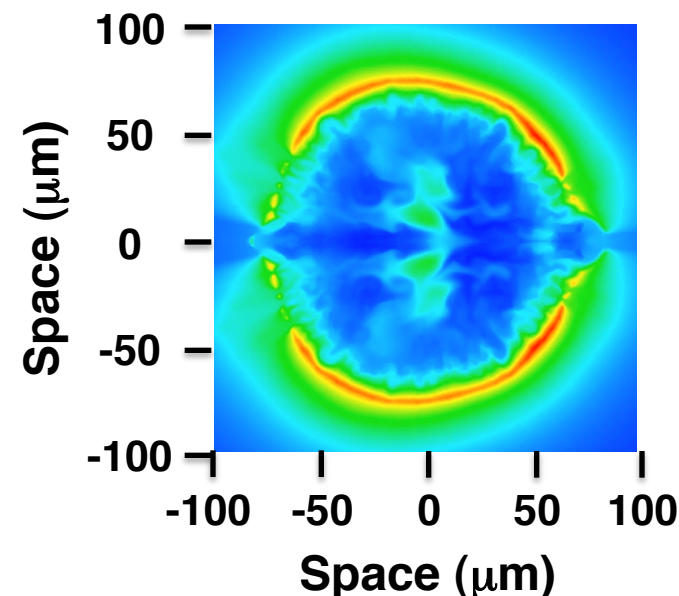
Diagnostics and targets can be optimized to study evolution of shock with time

- Change filtering to look at lower energies.
- Increase temporal coverage and resolution.
- Dope targets and perform spectroscopy.

1D and 2D radiography to observe shock emission and medium density.

Hydrodynamic evolution can be studied with perturbed implosions and medium

2D simulation with horizontal perturbation  
Radiated energy vs. space

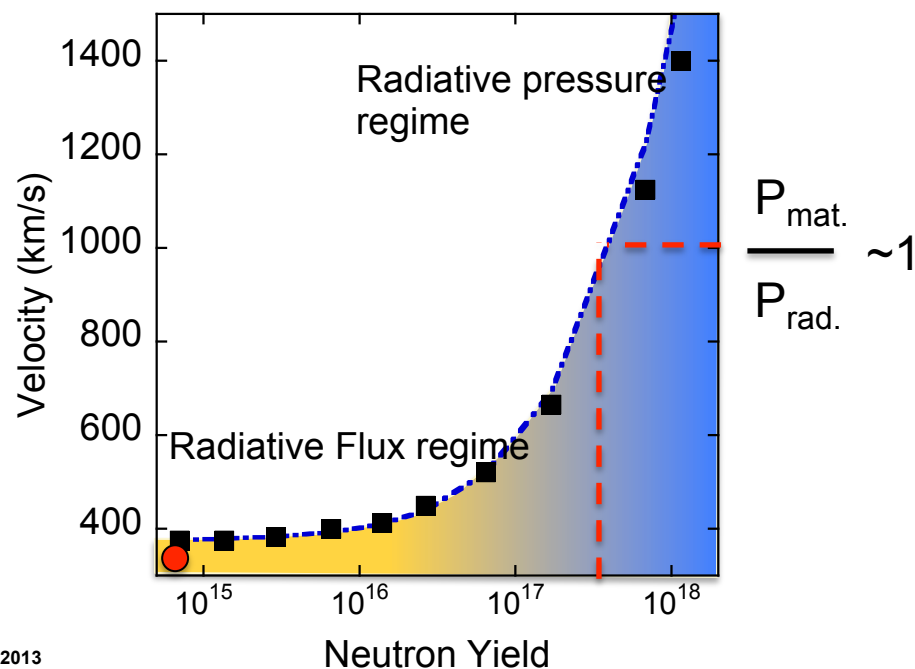
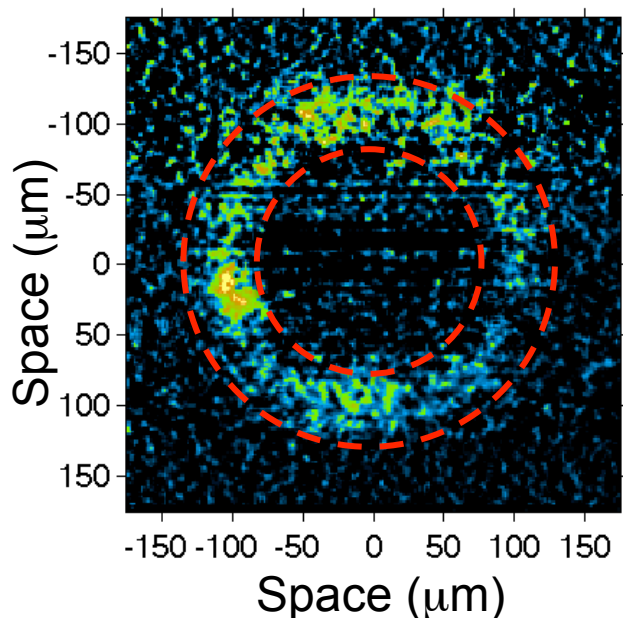


Target and drive can be optimized to study scaled hydrodynamic evolution.  
D. Ryutov *et al.* ApJ 518. 821-832(1999)  
S. Bouquet *et al.* HEDP, 6. 368-380(2010)



## Summary

- A spherical radiative shock wave propagating outwards at a lab frame velocity of 300 km/s into an in-falling medium, has been observed from the expansion phase of an integrated implosion experiment.
- The luminosity and velocity of the out going shock can be accurately diagnosed and agree with radiation hydrodynamic simulations.
- The dynamics of our implosion experiments may offer opportunities to study the evolution and morphology of young supernova remnants.



# Thanks to the NIF team!





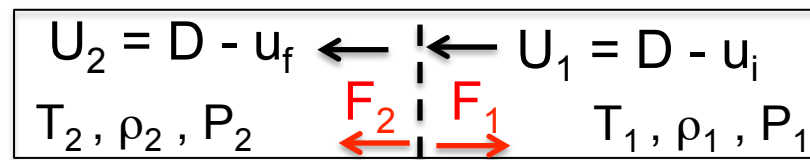
# NIC

The letters "NIC" are rendered in a bold, white, sans-serif font. A thin, white, curved line arches beneath the letters, starting under the 'N' and ending under the 'C'.

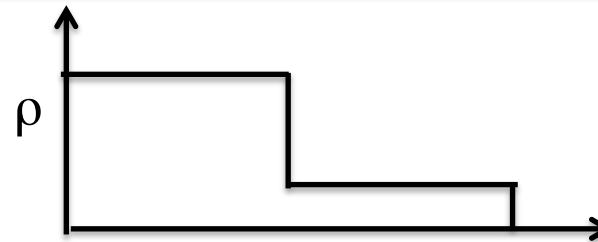
# Radiation transport can alter the up and downstream material properties changing shock front structure

- Mass, momentum and energy are conserved across the shock front.

Shock frame



$D, u_i, u_f$  lab frame velocity



$$\rho_2 U_2 = \rho_1 U_1$$

Mass

$$\rho_2 U_2^2 + P_2 = \rho_1 U_1^2 + P_1$$

Momentum

$$\rho_2 U_2 \left( e_2 + \frac{1}{2} U_2^2 + \frac{P_2}{\rho_2} \right) + F_2 = \rho_1 U_1 \left( e_1 + \frac{1}{2} U_1^2 + \frac{P_1}{\rho_1} \right) - F_1$$

Energy

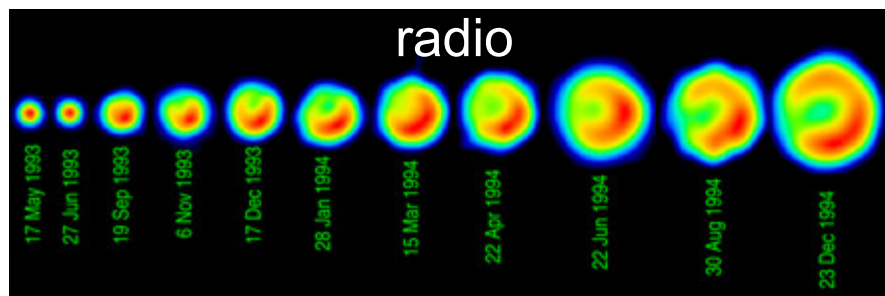
Hugoniot relations

- When the radiative flux  $F_1 = \sigma T_2^4 > \rho_0 U_1^3 / 2$  inflowing material energy flux, radiation energy flux must be considered.



# Prompt hard x-ray emission from supernova created by forward ejecta driven shock wave

Early high energy x-ray emission dominated by Bremsstrahlung



- Shell of ejecta drives shock into H-He CSM.
- High energy x-ray emission arises from forward shock.

Does physics from laboratory shock scale to supernova luminosity?

Scaling from SN to the laboratory

Detector	Day	Energy band	Luminosity (erg/s)
Roast	7	.1-2.4 keV	2.94E+39
Asca	29	1-10 keV	5E+39
OSSE	12	50-100 keV	5.5E+40
OSSE	28.5	50-100 keV	3E+40

Data from NIF	>9keV	3E+16
Simulation	>1keV	2.25E+19

$$L_{scaled} \propto Z^2 n_e n_i T^{1/2} Vol. \quad \text{Integral of Bremsstrahlung}$$

$$n_e = \left( \frac{Z\rho}{A} \right) \quad n_i = \left( \frac{\rho}{A} \right)$$

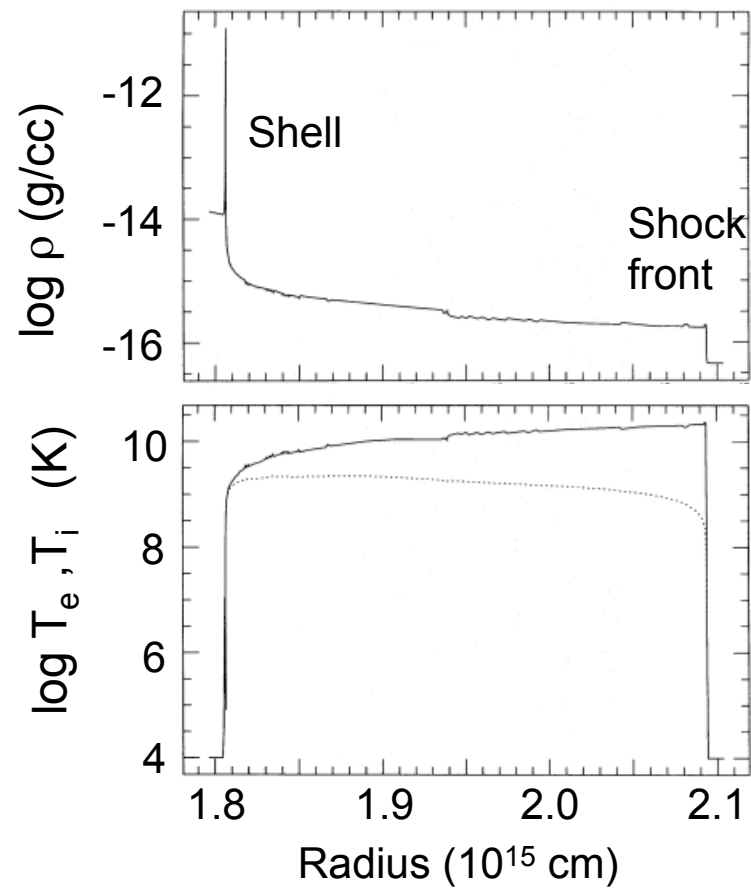
$$T^{1/2} \propto U_1 \propto \frac{R}{t} \quad Vol \propto R^3$$

Ratio of measured luminosities should equal ratio of scaled luminosities

# Correct order of magnitude for scaled luminosities

Stellar model of 1993J x-ray luminosity gives radius and density.

Ratio of measured to scaled luminosity approximately equal.



$$\Theta_M = \frac{L_{SN}}{L_{NIF}} \qquad \Theta_S = \frac{L_{SN-scaled}}{L_{NIF-scaled}}$$

$$\frac{\Theta_M}{\Theta_S} \approx 1$$

	R (m)	t (s)	ρ (g/cc)	A (mp)	Z
SN 1993	2.1E+13	1036800	3.17731E-16	1.3	1.1
NIF	0.00013	3.00E-10	10	6.5	2.5

$$\Theta_m = 2.44444E+21$$

$$\Theta_s = 4.23592E+20$$

$\Theta_m/Q_s$ 
5.770748066

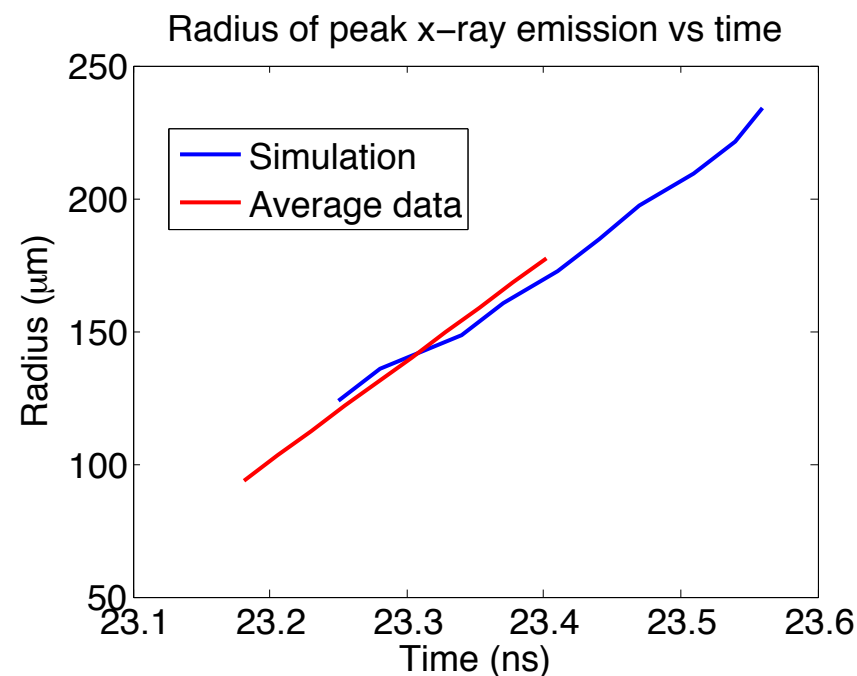
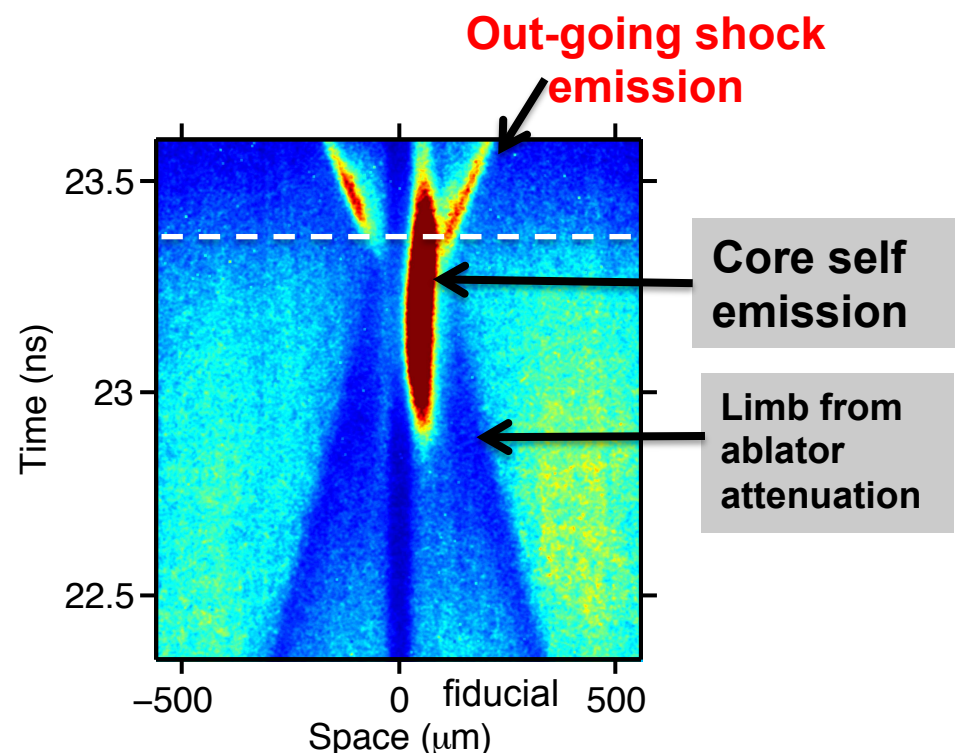
Laboratory experiment appears to capture the essential physics

C. Fransson, P. Lundquist and R. A. Chevalier, ApJ, 461:993-1008, 1996

# Different astrophysical regimes can be studied by modifying the target and diagnostics

Diagnostics can be optimized to study evolution of shock with time

- Filtering to look at lower energies.
- 1D and 2D radiography to observe shock emission and medium density.



Simulations from R. Olson